LAJSBA
LATIN AMERICAN JOURNAL OF SEDIMENTOLOGY AND BASIN ANALYSIS | VOLUME 29 (2) 2022, 83-95

APPLICABILITY OF CALCIMETRY IN LOW-CALCIUM CARBONATE SEDIMENTS

Cecilia G. Cantera [1], *Ivana Laura Ozán* [2]

[1] Laboratorio de Análisis Químicos Aplicados a las Geociencias, Departamento de Ciencias Geológicas, Facultad de Ciencias Exactas y Naturales, Universidad de Buenos Aires (UBA). Intendente Güiraldes 2160, C1428EHA Buenos Aires, Argentina. E-mail: ceciliacantera@gmail.com
[2] Consejo Nacional de Investigaciones Científicas y Técnicas – UBA. Instituto de Geociencias Básicas, Aplicadas y Ambientales de Buenos Aires. Intendente Güiraldes 2160, C1428EHA Buenos Aires, Argentina. E-mail: ivanal.ozan@gmail.com

ARTICLE INFO

Article history
Received July 15, 2022
Accepted October 3, 2022
Available online October 3, 2022

Handling Editor
José I. Cuitiño

Keywords
Non-calcareous sediments/soils
Pressure calcimetry
Detection/ Quantification limits
Loss-on-Ignition
Micromorphology

ABSTRACT

In Earth and Environmental Sciences, pressure calcimetry is probably the most efficient and fast method to determine calcium carbonate ($CaCO_3$) content in rocks, sediments and soils. However, measurements of low-$CaCO_3$ samples can be less reliable by calcimetry, depending on the instrument used. This problematic is particularly relevant for sediments and soils with low content of $CaCO_3$, very common in past and present lakes, soils and hydromorphic systems (*e.g.,* peatbogs, mires, wetlands), where $CaCO_3$ analysis contribute to understand water table changes, groundwater oscillation, ecology and wind-related processes, among others. In this context, this work presents a simple protocol to obtain accurate $CaCO_3$ determinations through pressure calcimetry in low-$CaCO_3$ samples (<4%), even though their $CaCO_3$ content falls below the limit of detection of the instruments. Calibration curves were first established with a $CaCO_3$ standard to calculate the critical value, detection limit and quantification limit, using two different pressure calcimeters. By considering these thresholds, a set of four natural samples with low-$CaCO_3$ content were measured by pressure calcimetry and also analyzed by Loss-on-Ignition and micromorphology. Results with 1 g of sample were lower than the detection limit. Accordingly, a gradual increase of sediment mass was applied until obtaining results above the quantification limit. The amount of $CaCO_3$ per g was thus inferred. Both calcimeters showed comparable results and high consistency with micromorphological observations. The $CaCO_3$ content calculated by Loss-on-Ignition showed slightly lower values, likely due to the loss of structural water and dehydroxylation of some minerals exposed to high temperature, affecting calculations of both organic and inorganic carbon.

INTRODUCTION

The $CaCO_3$ determinations are standard analysis in Geology, Environmental Sciences and Soil Sciences, among other disciplines. Although many methodologies have been developed to quantify $CaCO_3$ content, coulometric titration (*e.g.,* Engleman *et al.*, 1985; Rowell, 1994; Kassim, 2013; Elfaki *et al.*, 2016), oxidation by combustion (*e.g.,* Heiri *et al.*, 2001; Wang *et al.*, 2011, 2013), and CO_2

pressure measurement after acid neutralization (*e.g.,* Sherrod *et al.*, 2002; Stetson and Osborne, 2015) have been the most extended methods in Geosciences. These methods comprise low cost and time-consuming protocols, compared to more sophisticated techniques (*e.g.,* Zougagh *et al.*, 2005; Tatzber *et al.*, 2007; Gómez *et al.*, 2008; Li *et al.*, 2020). The $CaCO_3$ type crystallinity (*i.e.*, calcite, dolomite, aragonite), the expected content of $CaCO_3$, the presence of organo-mineral components mixed in natural samples and the required data precision will determine the most suitable methodology in each case.

The $CaCO_3$ determination by Loss-on-Ignition (LOI) is a gravimetric method based on the $CaCO_3$ decomposition by temperature which measures mass differences between combustion steps whose temperatures and durations vary significantly according to protocols (Dean, 1999; Heiri *et al.*, 2001; Santisteban *et al.*, 2004; Wang *et al.*, 2011, 2013; Martínez *et al.*, 2018). This method is indirect since combustion not only alters $CaCO_3$, but also other components that also affect the final weight. For instance, important limitations arise when samples present abundant clays (*e.g.,* illite, kaolinite, vermiculite, smectite), gypsum, oxyhydroxides (*e.g.,* goethite), or any other H_2O/OH-bearing mineral. The loss of structural water *s.l.* of such minerals, at 550 °C or even below, may generate an overestimation of mass differences (Moore and Reynolds, 1997; Heiri *et al.*, 2001; Sun *et al.*, 2009; Wang *et al.*, 2011).

On the other hand, the $CaCO_3$ estimation by calcimetry is based on the CO_2 pressure measurement after acid neutralization with HCl. Reaction occurs as follows:

$$CaCO_3 + 2\ HCl \rightarrow CO_2 + H_2O + CaCl_2$$

As observed with other methodologies, significant technical variations exist within calcimetry, including digital manometers with different types of glass chambers or the use of volumetric instruments such as the traditional Bernard or Scheibler calcimeters (Sherrod *et al.*, 2002; Horváth *et al.*, 2005). Independently of the instrument design, a well-known pitfall in calcimetry is the overestimation of $CaCO_3$ content in samples with abundant organic matter (Hieri *et al.*, 2001; Wang *et al.*, 2011). Beyond this limitation, which can be controlled by addition of $FeCl_2$ or $FeSO_4$ (Loeppert and Suarez, 1996; Sherrod *et al.*, 2002), it is noteworthy that the variety of chemical reactions taking place during acid neutralization inside the hermetic glass are better known than those produced under oxidizing conditions (LOI method) inside a furnace.

An important issue of any analytical determination derived from instrumental techniques is related to the limits of detection and quantification (Currie, 1995, 1999; ISO, 2000), information that is rarely provided by protocols. This is particularly important when analyzing low-$CaCO_3$ content sediments (*e.g.,* <4%), like the ones found in pedo-sedimentary and lake-core sequences (Dean, 1999; Zolitschka *et al.*, 2000; Bockheim and Douglass, 2006; Doberschütz *et al.*, 2014; Ozán *et al.*, 2019; Li *et al.*, 2020). In this context, the present work aims to present the critical value (L_C), the detection limit (L_D), and the quantification limit (L_Q) of two pressure calcimeters that could be considered representative of instruments used worldwide, in order to propose a simple protocol to determine the $CaCO_3$ content in natural samples with a low content of this compound, namely, below the L_D and L_Q of the instruments. In this regard, L_D and L_Q values were first calculated for both calcimeters and a series of essays were run with a pure salt pattern and natural samples. The $CaCO_3$ content in the latter was also analyzed by LOI, so inter-method and intra-method results are discussed, as well as the applicability and pitfalls of calcimetry in low-$CaCO_3$ content samples.

MATERIALS AND METHODS

Two pressure calcimeters were used to conduct the study: 1) the CALHH81, Netto S.E (series *N°0921-8697*, made in Argentina) (Fig. 1a), and 2) the Digital Gauge Calcimeter 2.3, Houston Mud Logging Supplies, LLC (series 4395, made in USA) (Fig. 1b). Instruments (hereafter referred as Netto and HMLS) were operated at room temperature (~20 °C) at the Chemical Laboratory of the Department of Geological Sciences at the University of Buenos Aires (Argentina).

The Netto calcimeter measures the CO_2 pressure generated from the dissolution of $CaCO_3$ contained in a dry sample (1 g) when adding 20% HCl solution (20 ml) by using a piezoresistive sensor. The reaction takes place in a hermetic acrylic container of 500 ml, placed in a metal press. The glass is connected to

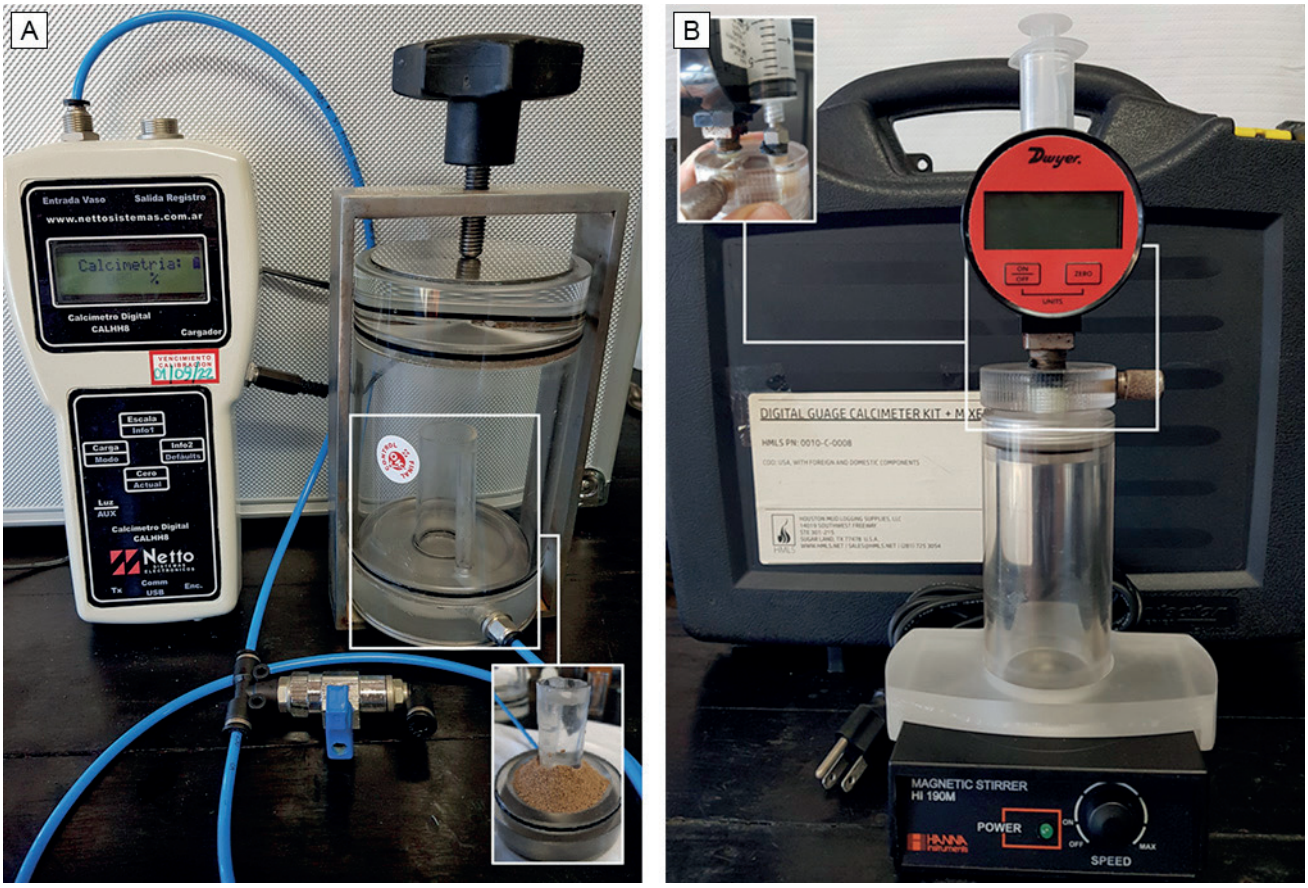

Figure 1. View of pressure calcimeters. **a)** CALHH81-Netto S.E ("Netto"), and **b)** Digital Gauge Calcimeter 2.3-Houston Mud Logging Supplies, LLC ("HMLS").

the sensor equipment through a three-month valve, using a thin tube (143 cm length and 4 mm diameter) (Fig. 1a). Dissolution processes occur when the acid is manually decompartmentalized and mixed with the sample. After reaction, gases are released through the third valve orifice. An internal auto-calibration converts pressure into percentage with a 0.1% precision. After ca. 45 seconds, measurements are stabilized, and gases can be released. The glass is then carefully washed and rinsed with milli-Q water. Once the instrument is turned on, an external calibration with 1 g of pure $CaCO_3$ is needed to set 100% concentration, whereas the auto-zero is established before each measurement.

In contrast to Netto, the HMLS design is alike others pressure calcimeters commercialized worldwide. Here, a digital manometer is attached to a hermetic acrylic container of 137 ml placed on a magnetic stir bar to favor the reaction. The HCl solution (10%, 20 ml) is injected with a luer lock syringe into the reaction chamber (Fig. 1a), where 1 g of dry sample is placed. After a 30-seconds measurement, gases are released. The glass is then carefully washed and rinsed with milli-Q water. A single external calibration is required to correlate the pressure value of the CO_2 (PSI) with the concentration (%) of $CaCO_3$ (precision 0.01 PSI). The auto-zero is stablished before each measurement.

External calibration curves

Instruments were calibrated using a $CaCO_3$ standard of analytic quality (99.7%), dried during 12 hours at 105 °C and stored in a desiccator with silica gel (same protocol was followed for dry natural samples). Different proportions (in triplicate) of pure salt (0; 0.005; 0.001; 0.05; 0.1; 0.25; 0.5; 0.75; 1 g) were used to build the curve. A precision balance of 0.0001 g was used to weigh the pure salt and natural samples. The statistical analysis and linear regression fit were performed with Origin 9.0 Pro software.

Critical Value, Detection limit and Quantification limit

Three parameters were calculated for each calibration curve (*i.e.*, L_C, L_D, L_Q) following criteria of the International Organization for Standardization (ISO) and the Upper Limit Approach (ULA), recommended by the International Union of Pure and Applied Chemistry (IUPAC).

The critical value (L_C) is the minimum significant value of an estimated net signal (or concentration), applied as a discriminator against background noise. The comparison of an estimated quantity with the L_C, such that the probability of exceeding L_C is no greater than α if the analyte is absent, allows making the decision whether the net signal (or concentration) is detected or not (Currie, 1995, 1999; ISO, 2000). Assuming the results have a normal distribution with known variance, the L_C can be described as:

$$L_C = z_{1-\alpha}\sigma_0 \quad (1)$$

where $z_{1-\alpha}$ is related to the (1-α) percentage point of the standard normal variable and σ_0 is the standard deviation of the blank. If the data have a normal distribution with a known variance and ν degrees of freedom, $z_{1-\alpha}$ must be replaced by the t distribution parameter ($t_{(1-\alpha,\nu)}$).

According to ISO (2000), this expression becomes:

$$L_C = t_{(1-\alpha,\nu)}\frac{\hat{\sigma}}{\hat{b}}\sqrt{\frac{1}{K}+\frac{1}{I\cdot J}+\frac{\bar{x}^2}{J\cdot\sum_{i=1}^{n}(x_i-\bar{x})^2}} \quad (2)$$

where $\hat{\sigma}$ is the estimated residual standard deviation of the calibration curve, $\hat{b}$ is the estimated value of the slope, K is the number of preparations for the actual state, I is the number of states (calibration standards) and J is the number of parallel measurements.

On the other hand, ULA (Mocák *et al.*, 1997, 2009; Vogelgesang and Hädrich, 1998), describes the L_C as:

$$L_C = t_{(n-2,1-\alpha)}\frac{\hat{\sigma}}{\hat{b}}\sqrt{1+\frac{1}{n}+\frac{\bar{x}^2}{\sum_{i=1}^{n}(x_i-\bar{x})^2}} \quad (3)$$

where n (equivalent to $I{\cdot}J$, see eq. 2) is the total number of measurements.

The minimum detectable value or detection limit (L_D) of the net signal (or concentration) is the value for which the false negative error is β, given L_C (or α) (Currie, 1995, 1999). It is the true net signal (or concentration) for which the probability that the estimated value does not exceed L_C is β. Mathematically, when the distribution is normal and the variance is known, the L_D is given as:

$$L_D = z_{1-\alpha}\sigma_0 + z_{1-\beta}\sigma_D \quad (4)$$

where σ_D is the standard deviation which characterizes the probability distribution of the signal when its true value is equal to L_D. In case the variance is constant, σ_D is equal to σ_D and, based on ν degrees of freedom, $z_{1-\alpha} + z_{1-\beta}$ must be replaced by $\delta_{(\alpha,\beta,\nu)}$, the non-centrality parameter of non-central-t distribution (Currie, 1995, 1999; ISO, 2000).

The expression for L_D described by ISO (2000) is:

$$L_D = \delta_{(\alpha,\beta,\nu)}\frac{\hat{\sigma}}{\hat{b}}\sqrt{\frac{1}{K}+\frac{1}{I\cdot J}+\frac{\bar{x}^2}{J\cdot\sum_{i=1}^{n}(x_i-\bar{x})^2}} \quad (5)$$

When $\alpha = \beta$, $\delta_{(\alpha,\beta,\nu)}$ is approximately equal to $2t_{(n-2,1-\alpha)}$. The expression for L_D suggested for the ULA is:

$$L_D = 2t_{(n-2,1-\alpha)}\frac{\hat{\sigma}}{\hat{b}}\sqrt{1+\frac{1}{n}+\frac{\bar{x}^2}{\sum_{i=1}^{n}(x_i-\bar{x})^2}} = 2L_C \quad (6)$$

Finally, the limit of quantification (L_Q) refers to the smallest net signal (or concentration), which can be quantitatively analyzed with a reasonable reliability by a given procedure (Currie, 1995, 1999). The ability to quantify is generally expressed in terms of the signal or analyte (true) value that will produce estimates having a specified relative standard deviation (RSD), commonly 10%. That is,

$$L_Q = 10\sigma_Q = 10\sigma_0 \quad (7)$$

where σ_Q is the standard deviation at that point and 10 is the multiplier, whose reciprocal equals the selected quantifying RSD. If σ_Q is known and constant, then σ_Q in eq. (7) can be replaced by σ_0.

The various approaches to the L_Q are somehow arbitrary. When using the ULA, the L_Q is described by three times the L_C:

$$L_Q = 3t(n-2{,}1-\alpha)\frac{\hat{\sigma}}{\hat{b}}\sqrt{\frac{1}{K}+\frac{1}{n}+\frac{\bar{x}^2}{\sum_{i=1}^{n}(x_i-\bar{x})^2}} = 3L_C \quad (8)$$

It is noteworthy that detection and quantification limits refer to the capabilities of the measurement process itself and are not associated with any particular outcome or result (Bernal and Guo, 2014). On the other hand, the detection decision is result-specific, since it is made by comparing the experimental result with the critical value used to make a posteriori estimation of the detection capabilities of the measurement process, while the limit of detection is used to make an a priori estimate (Bernal and Guo, 2014).

Natural samples

Four natural samples from the Western Pampas Dunefield, province of San Luis, Argentina, (Zárate and Tripaldi, 2012; Tripaldi and Zárate, 2016) were considered for analytical essays (*i.e.,* M3, M13, G1 and RC1). They correspond to Quaternary sediments recovered at different levels of aeolian sequences (*i.e.,* vegetated dunes) with low-intensity pedogenesis/diagenesis (Tripaldi and Forman, 2007, 2016; Tripaldi *et al.*, 2010, 2013; Forman *et al.*, 2014). Well-sorted, fine-grained sands composed of volcanic lithics fragments, volcanic glass shards, and feldspars dominate the lithology of these sands (Forman *et al.*, 2014; Tripaldi and Forman, 2016).

The clay fraction was measured by means of sedigraphy (Malvern Sedigraph). Structured thin sections for micromorphological descriptions and mineralogical optical quantification analyzed under a petrographic microscope (Zeiss, Axioplan 2) were also done at the same levels where the bulk samples used for calcimetry were taken (Stoops, 2003; Stoops *et al.*, 2010; Ozán *et al.*, 2019). Additional data concerning macroscopic characteristics of the sample (*i.e.,* texture, structure, colour, context) were also reported (Folk *et al.*, 1970; Munsell Color, 1994).

Pressure calcimetry in natural samples: After quartering, samples with concretions and/or aggregates were homogenised using a porcelain mortar. Since granulometry is <100 μm, the use of sieves was avoided. Samples were dried and weighted as mentioned above (see "External calibration curves").

The $CaCO_3$ content of natural samples was estimated with the two different pressure calcimeters, following the corresponding protocols (see above, Materials and Methods). Since the evaluated signals for 1 g of each sample were often lower than the L_D and/or L_Q, masses were increased gradually ("additional mass procedure") until reaching results (% $CaCO_3$) above the L_Q (the amount of sample in the Netto calcimeter was limited by the chamber design; Fig. 1a). At least four measurements were performed for each sample and an accurate $CaCO_3$ per g was then calculated.

Loss-on-Ignition in natural samples: Duplicate samples were ground with a porcelain mortar and weighted with a 0.001 g precision balance. About 3 g of sample was placed in porcelain crucibles a) to dry in oven for 12 hours (105 °C) and burnt in furnace at b) 550 °C and then c) 950 °C, for 2 hours in each combustion step (Heiri *et al.*, 2001). Mass differences (in percentages) between each step gave the content of a) Water loose, b) Organic Matter, and c) $CaCO_3$ (after applying the 1.36 convert factor). Calculation of the Organic Matter (%) and the $CaCO_3$ (%) followed these equations (Heiri *et al.*, 2001):

$$\mathrm{LOI}_{550} = \frac{DW_{105}-DW_{550}}{DW_{105}} \cdot 100 \quad (9)$$

$$\mathrm{LOI}_{950} = \frac{DW_{550}-DW_{950}}{DW_{105}} \cdot 100 \cdot 1.36 \quad (10)$$

where *DW* represents the dried sample weight at different steps. Roughly, authors report an error of about 2% for LOI estimations.

The statistical analysis for the comparison of LOI_{950} and calcimetry results was conducted using a parametrical Two-way ANOVA test, followed by a Bonferroni posttest.

RESULTS

Calibration curves: L_C, L_D and L_Q determinations

The linear regression for both calibration curves (Fig. 2) shows a determination coefficient (R^2) above 0.997, which means that this model explains the 99.7% of the variance of these results (Table 1). In the case of HMLS, the linear fit is slightly better than the one for Netto, since the R^2 value is not only higher

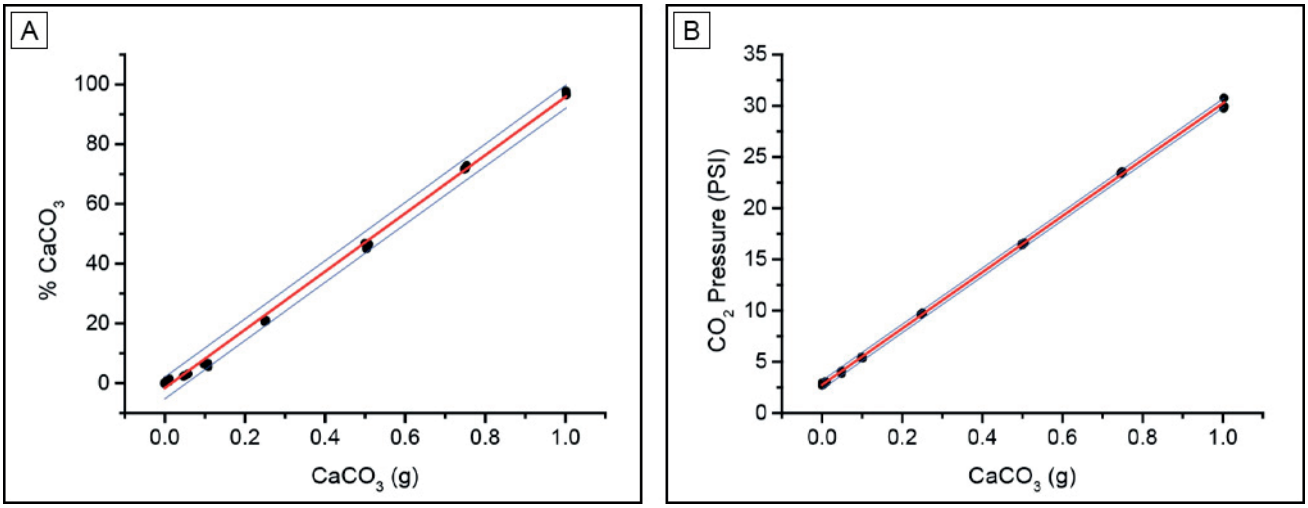

Figure 2. External linear calibration curves (red), and 95% prediction band (blue) for **a)** Netto and **b)** HMLS calcimeters.

but also residuals are normally distributed (Table 1, Fig. 3b). On the other hand, the residual plot for Netto shows a non-random pattern presenting a trend towards positive values for the low and high $CaCO_3$ extremes, respectively (Fig. 3a).

The comparison of L_C and L_D with both instruments shows no significant differences between ISO and ULA methods (Table 2). Limits calculated with Netto are nearly three times higher than those calculated with HMSL. In this sense, the Netto L_C, L_D and L_Q are 3.1%, 6.2% and 9.3%, respectively, whereas in HMSL, those parameters are 1.2%, 2.5% and 3.7%, respectively (Table 2). Thus, the latter equipment shows better performance for low $CaCO_3$ content determinations.

Natural samples: relevant characteristics and LOI determinations

The analyzed sandy sediments present a low organic matter content, between 1.5-2.7% and a variable proportion of clay fraction (0.5-4.3%). Concerning the $CaCO_3$ content determined, results show values between 0.5-1.5%.

Optical estimation of mineral composition (Table 3) shows that M3 and M13 samples mainly present plagioclase, followed by K-feldspar, lithic fragments (mainly volcanic), volcanic glass shards, and quartz, among other minor minerals. Sample G1 is mainly composed by lithics followed by volcanic glass, quartz, K-felspar, and opaques; whereas RC1 is dominated by K-felspar, opaques, volcanic glass, and plagioclase.

Broadly, the well-sorted fine sands observed through the micromorphological examination of M3 supports the aeolian origin of the deposit (Forman *et al.*, 2014; Tripaldi and Forman, 2016), with rare organic matter and the occurrence of diagenetic features represented by formation of authigenic clay minerals (*e.g.*, illite) and the precipitation of

	Intercept				Slope				Statistics
	Value	Standard Error	95% LCL	95% UCL	Value	Standard Error	95% LCL	95% UCL	R^2
Netto	-1.61262	0.43413	-2.50674	-0.71851	97.44073	0.94543	95.49358	99.38788	0.99756
HMLS	2.75690	0.04851	2.65699	2.8568	27.47344	0.10584	27.25546	27.69141	0.99961

LCL: Low Confidence Limit. UCL: Upper Confidence Limit.

Table 1. Linear fit parameters of calibration curves for both calcimeters measured by LOI and pressure calcimetry with Netto and HMSL calcimeters.

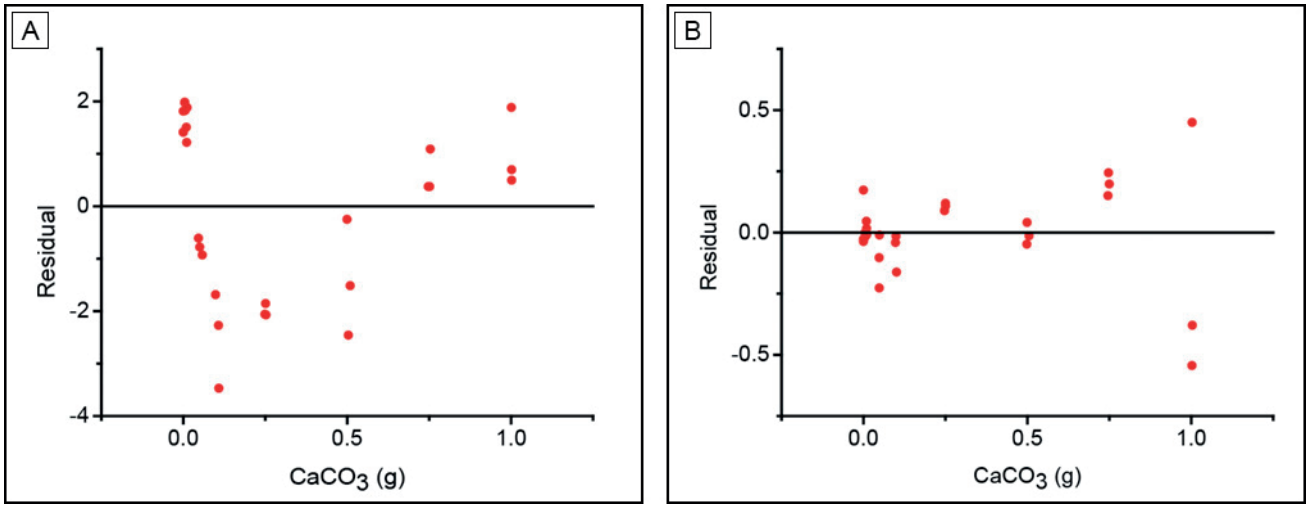

Figure 3. Residual plots for **a)** Netto and **b)** HMLS calcimeters.

amorphous Fe/Mn oxides (*e.g.,* goethite) derived from the volcanic glass weathering (Fig. 4a). Sample M13 is similar to M3, but the thin section does not register the presence of organic matter remains, whereas it shows a crystallithic b-fabric, suggesting the presence of $CaCO_3$ embedded in the matrix. Indeed, abundant nodules, stains, coatings, and hypocoatings of $CaCO_3$, some of them with signals of dissolution and re-precipitation, are also observed (Fig. 4b).

In the case of G1, the micromorphology shows a relatively finer deposit with a lack of organic matter but abundant amorphous $CaCO_3$ as stains, nodules, infillings, accretions, and hypocoatings (Fig. 4d). In situ mineral weathering, particularly around volcanic glass (*e.g.,* goethite) is also registered (Fig. 4e). Alike G1, RC1 sample shows a loamy deposit (Fig. 4f), which includes silty-clay void infillings and frequent detritic clay domains with speckled/crystallithic b-fabric (Fig. 4g). Rare plant tissue remains are observed as pseudomorph of Fe/Mn oxides and the undifferentiated b-fabric (Fig. 4f) may suggest the presence of highly degraded organic matter (*i.e.,* humus).

$CaCO_3$ by pressure calcimetry in natural samples by applying the "additional mass procedure": The amount of % $CaCO_3$ per g of sediment sample considered an "accurate" result is an average of % $CaCO_3$ per g of measurements which yielded values above the L_Q. Thus, reliable results are observed in three samples using both instruments, but not in M3. The high L_C value calculated for Netto (3.1%), prevented this calcimeter to detect the very low content of $CaCO_3$ in sample M3, not even with 12 g, the maximum volumetric limit of the glass (Fig. 1a). Similarly, the L_D could not be reached with the

			ISO		ULA	
		1-α	g $CaCO_3$	% $CaCO_3$	g $CaCO_3$	% $CaCO_3$
Netto	L_C	0.95	0.0302	3.0	0.0311	3.1
	L_D	0.95	0.0598	6.0	0.0621	6.2
	L_Q				0.0932	9.3
HMLS	L_C	0.95	0.0135	1.3	0.0123	1.2
	L_D	0.95	0.0266	2.7	0.0247	2.5
	L_Q				0.0370	3.7

Table 2. Comparison of L_C, L_D and L_Q determined by ISO and ULA for both calcimeters.

Sample	Depositional context and broad sedimentological characterization	Relevant micromophological features	Major mineralogy (>5%)	% Organic matter (LOI)	% $CaCO_3$ (LOI)
M3 33°58'20.04"S 65°35'19.14"W	Aeolian succession. Sampled interval: 140-150 cm depth. Silty sand texture. Single grain deposit (7.5YR 5/3, brown). Clay content: 0.54%.	- Microstructure: Massive. - Porosity: ~5-10%. - Coarse/Fine ratio$_{(50\mu m)}$: 95/5. - Related distribution: monic. - B-fabric: granostriated. - Organic matter remains: rare/ occasional plan tissues as Fe/Mn oxide pseudomorphs. - Diagenesis: mineral weathering as authigenic clay and Fe/Mn precipitations, particularly around volcanic glass (Fig. 4a).	Pl 39%, Kfs 25%, Lith 12%, V. gl 8%, Qtz 8%.	1.5 ± 0.2	0.49 ± 0.06
M13 33°58'20.04"S 65°35'19.14"W	Aeolian succession. Sampled interval: 760-770 cm depth. Silty sand texture. Single grain deposit with few concretions (7.5YR 6/2, pinkish grey). Clay content: 1.42%.	- Microstructure: Massive. - Porosity: 5-10%. - Coarse/Fine ratio$_{(50\mu m)}$: 95/5. - Related distribution: monic. - B-fabric: crystallithic, speckled, granostriated. - Organic matter remains: not observed. - Diagenesis: abundant nodules, stains, coatings and hypocoatings of $CaCO_3$. Dissolutions and re-precipitation of $CaCO_3$ (micritic). Few Fe/Mg stains (Figs. 4b and 4c).	Pl 42%, Kfs 22%, Qtz 11%, V. gl 10%.	1.94 ± 0.02	0.77 ± 0.07
G1 34°25'54.48"S 65°48'12.90"W	Aeolian succession. Sampled interval: 0-10 cm depth. Silty sand texture. Massive/ compact structure (5Y 6/1, grey). Clay content: 3.75%.	- Microstructure: Massive. - Porosity: 15-20%. - Coarse/Fine ratio$_{(50\mu m)}$: 65/35. - Related distribution: monic, gerufic. - B-fabric: crystallithic. - Organic matter remains: not observed. - Diagenesis: abundant $CaCO_3$ as stains, nodules, embedded in matrix, as fillings, accretions and hypocoatings. In situ mineral weathering, particularly around volcanic glass (Figs. 4d and 4e).	Lith 38%, V. gl 18%, Op 13%, Qtz 12%, Kfs 10%, Pl 5%.	2.69 ± 0.08	1.5 ± 0.2
RC1 33°50'21.19"S 65°14'37.16"W	A-C soil horizon, aggradational soil profile, (parent material: aeolian sands). Sampled interval: 20-30 cm depth. Silty sand texture. Single grain deposit with few concretions (5YR 5/3, reddish brown). Weakly structured subangular blocks. Clay content: 4.29%.	- Microstructure: Massive. - Porosity: 5-10%. - Coarse/Fine ratio$_{(50\mu m)}$: 70/30. - Related distribution: enaulic. B-fabric: undifferentiated, slightly granostriated. - Organic matter remains: rare highly weathered plant tissues as pseudomorph of Fe/Mn oxides. - Diagenesis: partially preserved silty-clay infilling. Frequent detritic/ inherited clay domains with speckled/ striated/ crystallithic b-fabric (Figs. 4f and 4g).	Kfs 36%, Op 26%, V. gl 11%, Qtz 11%, Am 6%	1.770 ± 0.005	1.1 ± 0.1

Table 3. Natural samples under study. Data expressed as mean ± standard deviation of duplicate samples. Lith = lithics; Pl = plagioclase; Kfs = K-felspar; V. gl = volcanic glass; Qzt = quartz; Op = opaques; Am = amphiboles.

HMSL for 12 g of sample M3 because a technical limitation of the instrument.

DISCUSSION

First, two main relevant issues arise from the calculation of the L_C, L_D and L_Q values: 1) HMLS is a more sensitive calcimeter, thus showing lower values for these parameters, and 2) instruments do not accurately detect $CaCO_3$ content below their L_D, namely, 2.5% (HMLS) and 6% (Netto) (Table 2), so results challenge data robustness for low-$CaCO_3$ content samples. The more accurate results obtained with HMLS calcimeter are probably related to its smaller reaction chamber and the manometer being directly attached to the glass, a fact that simplifies the equipment by avoiding internal calibrations that may add another source of error. It is important to outline here that both instruments display a result even when measurements fall below the L_D, so users can obtain unreliable measurements if L_C, L_D and L_Q are unknown.

Pressure calcimetry measurements with 1 g of natural sample were lower than L_Q values, so a higher mass of sediment was gradually added until obtaining results above that limit (9.3% and 3.7% for Netto and HMLS calcimeters, respectively) (Table 2). Consequently, the amount of $CaCO_3$ corresponding to 1 g of sample was inferred (Table 5). This simple procedure proved to be successful in obtaining reliable results. Thus, in the case of the Netto instrument, if the expectation of $CaCO_3$ content is below 9.3% (L_Q), it is recommended to add ~10 g of sample and then normalize the result to 1 g. In the same way, with instruments like HMLS, which are more representative of worldwide designs, when samples with $CaCO_3$ content below 3.7% are expected, ~4 g samples should be used to obtain accurate values. Whereas this procedure increases the scope of the calcimetry methodology, the fact that it requires a high amount of sample implies a disadvantage for some studies, like limnological analyses, where coring gives low-mass samples.

Despite of differences concerning instrumental designs and their L_C/ L_D/ L_Q thresholds (Fig. 1, Table 2), both calcimeters yielded similar results of $CaCO_3$ in natural samples, though the very low $CaCO_3$ content of M3 could not be measured by any instrument, not even by the "additional mass procedure". Interestingly, micromorphological analysis did not show the presence of $CaCO_3$ on M3, therefore, the lack of accurate measurements in calcimetry could be related to a "real" absence of $CaCO_3$ in this sample. On the other hand, the abundance of $CaCO_3$ (estimated qualitatively) in thin sections of M13, G1 and RC1 samples support the amount of $CaCO_3$ content determined by calcimetry (Table 3).

Comparations between calcimetry results and the LOI method indicate rather similar values between both techniques (Table 5), except for G1. For M3 sample (undetectable in calcimetry), a ~0.5% of $CaCO_3$ was determined by LOI. However, as mentioned, the absence of $CaCO_3$ in the thin section may suggest that the value is not reliable for the method and/ or it is a consequence of other processes that occurs with burning, such as mineral water loss and mineral dehydroxylation at temperatures above 550 °C (*e.g.,* Moore and Reynolds, 1997; Wang *et al.*, 2011).

Even though non-significant differences in $CaCO_3$ content are observed in M13 and RC1 samples comparing the two methods (Table 5), slightly lower values in LOI (~23%) could be attributed to an overestimation of organic matter by LOI determinations, a fact that later impacts on $CaCO_3$ estimations (eq. 10). Similar arguments may explain the significant difference between calcimetry and LOI $CaCO_3$ estimations obtained for G1 sample, which yielded a below-50% value in LOI (Table 5) (*c.f.*, Li *et al.*, 2020). Here, while LOI analysis shows a relatively higher amount of organic matter compared to the other samples, micromorphology does not register the presence of any tissue remain not highly degraded organic matter such as humus. In addition, G1 sample presents the highest percentages of volcanic glass, whose weathering subproduct could be assigned to goethite, a mineral that suffer dehydroxylation above 300 °C (Sun *et al.*, 2009; Gialanella *et al.*, 2010). Indeed, geochemical analyses applied on the volcanic glass of the region supports the formation of such oxyhydroxide (Toms *et al.*, 2004; Tripaldi *et al.*, 2010).

In sum, pressure calcimetry is a fast $CaCO_3$ determination method (over 20 samples can be run in one hour work) with reliable results if the L_C, L_D and L_Q are calculated, as they are highly significative values for users. Furthermore, this analysis shows that when low-$CaCO_3$ content samples are under study, increasing the mass of sediments may help improve the sensibility of the instrument. Calcimetry results

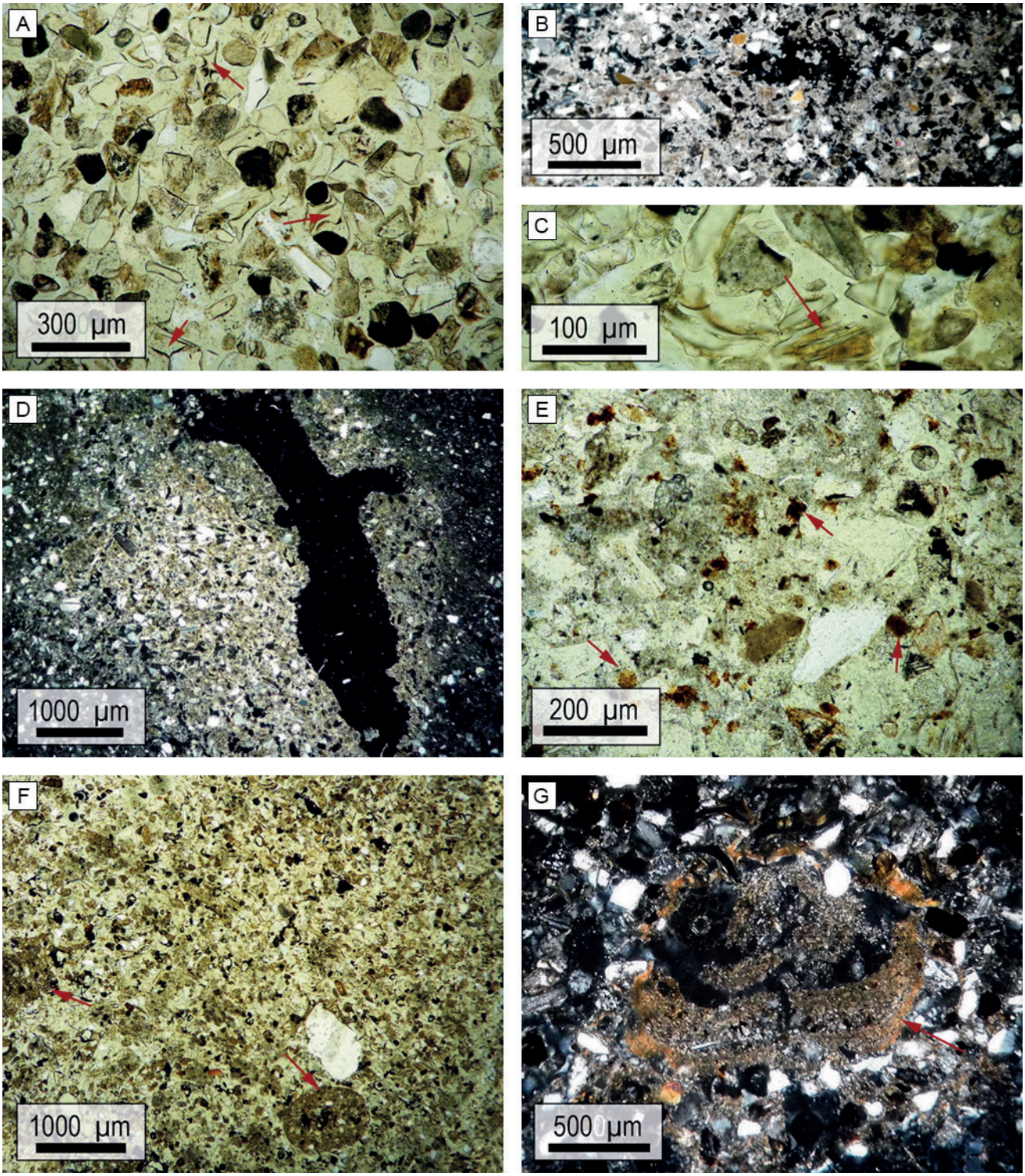

Figure 4. Microphotographs of structured thin sections corresponding to the four analyzed samples. **a)** Sample M3: massive, well sorted deposit of fine sands mainly represented by volcanic glass shards -indicated with red arrows- and highly altered lithics (Plane Polarized Light -PPL-). **b)** Sample M13: micritic $CaCO_3$ embedded in the matrix (Crossed Polarized Light -XPL-). **c)** Close up of sample M13: Fe-oxide (*e.g.*, goethite) because of in situ volcanic glass weathering (PPL). **d)** Sample G1: $CaCO_3$ hypocoating with some Fe/Mn-oxide stains; crystallithic b-fabric (XPL). **e)** Close up of sample G1: Fe-Mn-oxide nodules (red arrows), stains and coatings around particles (in situ mineral weathering) (PPL). **f)** Sample RC1: well sorted silty sand deposit, undifferentiated b-fabric, and signals of soil fauna activity -pointed by red arrows- (PPL). **g)** Detail of sample RC1: void coating/hypocoating of silty/clay, with crystallithic b-fabric (XPL).

	Netto			HMLS			
	g	% $CaCO_3$	% $CaCO_3$ per g	g	PSI	% $CaCO_3$	% $CaCO_3$ per g
M3	1.0079	0.00	0.0	1.0003	2.84	0.3	0.3
	3.9777	0.20	0.1	3.9838	2.90	0.5	0.1
	7.9505	0.40	0.1	7.9795	3.15	1.4	0.2
	11.9491	0.00	0.0	11.9559	3.11	1.3	0.1
			<3.1				<2.5
M13	0.9892	0.6	0.6	0.9909	2.98	0.8	0.8
	3.9791	2.4	0.6	1.9770	3.36	2.2	1.1
	7.9364	6.3	0.8	2.9649	3.72	3.5	1.2
	11.9115	10.50	0.9	3.9745	3.92	4.2	1.1
			0.9				1.1
G1	0.9923	1.90	1.9	0.9797	3.75	3.6	3.7
	3.9394	10.50	2.7	1.9857	4.67	6.9	3.5
	7.8605	24.30	3.1	2.9862	5.72	10.8	3.6
	11.7204	40.50	3.5	3.9177	6.51	13.6	3.5
			3.1 ± 0.4				3.5 ± 0.1
RC1	0.9820	1.30	1.3	0.9833	3.08	1.2	1.2
	3.9639	2.40	0.6	1.9737	3.10	1.2	0.6
	7.8911	5.30	0.7	2.9642	3.43	2.4	0.8
	11.8319	10.80	0.9	4.0023	3.77	3.7	0.9
			0.9				0.9

Table 4. Pressure calcimetry by Netto and HMSL calcimeters, applying the "additional mass procedure".

Sample	% $CaCO_3$		
	Pressure calcimetry		LOI
	Netto calcimeter	HMLS calcimeter	
M3	<3.1	<2.5	0.49 ± 0.06
M13	0.9	1.1	0.77 ± 0.07
G1	3.1 ± 0.4	3.5 ± 0.1	1.5 ± 0.2**
RC1	0.9	0.9	1.1 ± 0.1

Table 5. Synthesis of $CaCO_3$ content measured by LOI and pressure calcimetry with Netto and HMSL calcimeters. Significant differences between methods are given by two asterisks with a P value less than 0.01.

in the set of natural samples also show consistency with micromorphological analyses and, except for a few differences, LOI method.

CONCLUSIONS AND RECOMMENDATIONS

A simple protocol to obtain robust $CaCO_3$ determinations through pressure calcimetry in low-$CaCO_3$ samples (<4%), even though their $CaCO_3$ content falls below the limit of detection of the instruments, was validated by mean of calculations of the critical values (L_C), detection limit (L_D), and quantification limit (L_Q) for two different pressure calcimeter instruments. Then, a set of four natural samples with low-$CaCO_3$ content were measured with both calcimeters to prove the utility of such calculations. The L_C, L_D and L_Q (95% confidence) were 1.2%, 6.2% and 9.3%, respectively, for the Netto instrument (Argentina); and 1.2%, 2.5% and 3.7%, for the HMLS instrument (USA),

respectively. Determinations of $CaCO_3$ by LOI and micromorphological examinations were also conducted to expand the discussion of calcimetry results.

Since $CaCO_3$ content in natural samples was below the L_Q calculated for pressure calcimeters, a simple "additional mass procedure" was conducted to obtain results above the L_Q. Estimations of $CaCO_3$ per g were afterwards recalculated. This analysis derived in the need of including 10 g and 4 g, for Netto-like and HMLS-like instruments, respectively, in order to ensure accurate results.

Both calcimeters showed comparable results for natural samples and high consistency with micromorphological observations. In contrary, the latter analysis did not support the organic matter estimation by LOI (which could affect, in turn, $CaCO_3$ estimations), nor the presence of $CaCO_3$ in sample M3.

Acknowledgements

We first thanks Diego Kietzmann, who provided us to the HSML calcimeter for essays, and Sebastián Oriolo for his general comments about the manuscript. We are also grateful to Germán Fontana and Pablo Pohl (Netto company) for kindly sharing information and ideas about the equipment. Comments of reviewers Dra. A. Mehl and Dra. F. Mari, and editors undoubtedly helped improving this work. The analyzed natural samples were collected and analyzed under the project FONCyT-PICT2428 (Argentina).

REFERENCES

Bernal, E., and Guo, X. (2014). Limit of detection and limit of quantification determination in gas chromatography. *Advances in gas chromatography*, 3(1): 57-63.

Bockheim, J.G., and Douglass, D.C. (2006). Origin and significance of calcium carbonate in soils of southwestern Patagonia. *Geoderma*, 136(3-4): 751-762.

Currie, L.A. (1995). Nomenclature in evaluation of analytical methods including detection and quantification capabilities (IUPAC Recommendations 1995). *Pure and Applied Chemistry*, 67(10): 1699-1723.

Currie, L.A. (1999). Nomenclature in evaluation of analytical methods including detection and quantification capabilities:(IUPAC Recommendations 1995). *Analytica Chimica Acta*, 391(2): 105-126.

Dean, W.E. (1999). The carbon cycle and biogeochemical dynamics in lake sediments. *Journal of Paleolimnology*, 21(4): 375-393.

Doberschütz, S., Frenzel, P., Haberzettl, T., Kasper, T., Wang, J., Zhu, L., Daut, G., Schwalb, A., and Mäusbacher, R. (2014). Monsoonal forcing of Holocene paleoenvironmental change on the central Tibetan Plateau inferred using a sediment record from Lake Nam Co (Xizang, China). *Journal of Paleolimnology*, 51(2): 253-266.

Elfaki, J.T., Gafei, M.O., Sulieman, M.M., and Ali, M.E. (2016). Assessment of calcimetric and titrimetric methods for calcium carbonate estimation of five soil types in central Sudan. *Journal of Geoscience and Environment Protection*, 4: 120-127.

Engleman, E.E., Jackson, L.L., and Norton, D.R. (1985). Determination of carbonate carbon in geological materials by coulometric titration. *Chemical Geology*, 53(1-2): 125-128.

Folk, R.L., Andrews, P.B., and Lewis, S.W. (1970). Detrital sedimentary rock classification and nomenclature for use in New Zealand, New Zealand. *Journal of Geology and Geophysics*, 13: 937-968.

Forman, S.L., Tripaldi, A., and Ciccioli, P.L. (2014). Eolian sand sheet deposition in the San Luis paleodune field, western Argentina as an indicator of a semi-arid environment through the Holocene. *Palaeogeography, Palaeoclimatology, Palaeoecology*, 411: 122-135.

Gialanella, S., Girardi, F., Ischia, G., Lonardelli, I., Mattarelli, M., and Montagna, M. (2010). On the goethite to hematite phase transformation. *Journal of Thermal Analysis and Calorimetry*, 102(3): 867-873.

G**ó**mez, C., Lagacherie, P., and Coulouma, G. (2008). Continuum removal versus PLSR method for clay and calcium carbonate content estimation from laboratory and airborne hyperspectral measurements. *Geoderma*, 148(2): 141-148.

Heiri, O., Lotter, A.F., and Lemcke, G. (2001). Loss on ignition as a method for estimating organic and carbonate content in sediments: reproducibility and comparability of results. *Journal of Paleolimnology*, 25(1) :101-110.

Horváth, B., Opara-Nadi, O., and Beese, F. (2005). A simple method for measuring the carbonate content of soils. *Soil Science Society of America Journal*, 69(4): 1066-1068.

ISO 11843-2:2000. (2000). Capability of detection – Part 2: Methodology in the linear calibration case. In *International Organization for Standardization*. Corrigendum: ISO 11843-2/Cor1:2007: 24.

Kassim, J.K. (2013). Method for estimation of calcium carbonate in soils from Iraq. *International Journal of Environment*, 1(1): 9-19.

Li, N., Sack, D., Sun, J., Liu, S., Liu, B., Wang, J., Gao, G., Li, D., Song, Z., and Jie, D. (2020). Quantifying the carbon content of aeolian sediments: Which method should we use? *Catena*, 185: 104276.

Loeppert, R.H., and Suarez, D.L. (1996). Carbonate and gypsum. *Methods of soil analysis: Part 3 Chemical Methods*, 5: 437-474.

Martínez, J.M., Galantini, J.A., Duval, M.E., López, F.M., and Iglesias, J.O. (2018). Estimating soil organic carbon in Mollisols and its particle-size fractions by loss-on-ignition in the semiarid and semihumid Argentinean Pampas. *Geoderma Regional*, 12: 49-55.

Mocák, J., Bond, A.M., Mitchell, S., and Schollary, G. (1997). A Statistical Overview of Standard (IUPAC and ACS) and New Procedures for Determining the Limits of Detection and Quantification: Application to Voltammetric and Stripping Techniques. *Pure Applied Chemistry*, 69: 297-328.

Mocák, J., Janiga, I., and Rábarobá, E. (2009). Evaluation of IUPAC limit of detection and iso minimum detectable value

electrochemical determination of lead. *Nova Biotechnologica*, 9(1): 91-100.

Moore, D.M., and Reynolds Jr, R.C. (1997). *X-ray Diffraction and the Identification and Analysis of Clay Minerals*. Second edition. Oxford University Press (OUP). 332 pp.

Munsell Color (1994). *Munsell Soil Color Charts*. Macbeth Division of Kollmargen Instruments Corporation. New Windsor, New York. 28 pp.

Ozán, I.L., Méndez, C., Oriolo, S., Orgeira, M.J., Tripaldi, A., and Vásquez, C.A. (2019). Depositional and post-depositional processes in human-modified cave contexts of west-central Patagonia (Southernmost South America). *Palaeogeography, Palaeoclimatology, Palaeoecology*, 532: 109268.

Rowell, D.L. (1994). *Soil Science: Methods and Applications*. Prentice Hall, Harlow. 368 pp.

Santisteban, J.I., Mediavilla, R., Lopez-Pamo, E., Dabrio, C.J., Zapata, M., Garcia, M., Castan, S., and Martínez-Alfaro, P.E. (2004). Loss on ignition: a qualitative or quantitative method for organic matter and carbonate mineral content in sediments? *Journal of Paleolimnology*, 32(3): 287-299.

Sherrod, L.A., Dunn, G., Peterson, G.A., and Kolberg, R.L. (2002). Inorganic carbon analysis by modified pressure-calcimeter method. *Soil Science Society of America*, 66: 299–305.

Stetson, S.J., and Osborne, S.L. (2015). Further modification of pressure-calcimeter method for soil inorganic carbon analysis. *Soil Science and Plant Analysis*, 46(17): 2162-2167.

Stoops, G. (2003). *Guidelines for Analysis and Description of Soil and Regolith Thin Sections*. Soil Science Society of America, Madison. 185 pp.

Stoops, G., Marcelino, V., and Mees, F. (2010). *Interpretation of Micromorphological Features of Soil and Regoliths*. Elsevier, Amsterdam. 720 pp.

Sun, H., Nelson, M., Chen, F., and Husch, J. (2009). Soil mineral structural water loss during loss on ignition analyses. *Canadian Journal of Soil Science*, 89(5): 603-610.

Tatzber, M., Stemmer, M., Spiegel, H., Katzlberger, C., Haberhauer, G., and Gerzabek, M.H. (2007). An alternative method to measure carbonate in soils by FT-IR spectroscopy. *Environmental Chemistry Letters*, 5(1): 9-12.

Tripaldi, A., and Forman, S.L. (2007). Geomorphology and chronology of Late Quaternary dune fields of western Argentina. *Palaeogeography, Palaeoclimatology, Palaeoecology*, 251(2): 300-320.

Tripaldi, A., and Forman, S.L. (2016). Eolian depositional phases during the past 50 ka and inferred climate variability for the Pampean Sand Sea, western Pampas, Argentina. *Quaternary Science Reviews*, 139: 77-93.

Tripaldi, A., and Zárate, M.A. (2016). A review of Late Quaternary inland dune systems of South America east of the Andes. *Quaternary International*, 410: 96-110.

Tripaldi, A., Ciccioli, P.L., Alonso, M.S., and Forman, S.L. (2010). Petrography and geochemistry of late Quaternary dune fields of western Argentina: Provenance of aeolian materials in southern South America. *Aeolian Research*, 2(1): 33-48.

Tripaldi, A., Zárate, M.A., Forman, S.L., Badger, T., Doyle, M.E., and Ciccioli, P. (2013). Geological evidence for a drought episode in the western Pampas (Argentina, South America) during the early–mid 20th century. *The Holocene*, 23(12): 1731-1746.

Toms, P., King, M., Zárate, M., Kemp, R., and Foit, F. (2004). Geochemical characterization, correlation, and optical dating of tephra in alluvial sequences of central western Argentina. *Quaternary Research*, 62(1): 60-75.

Vogelgesang, J., and Hädrich, J. (1998). Limits of detection, identification and determination: a statistical approach for practitioners. *Accreditation and quality assurance*, 3(6): 242-255.

Wang, Q., Li, Y., and Wang, Y. (2011). Optimizing the weight loss-on-ignition methodology to quantify organic and carbonate carbon of sediments from diverse sources. *Environmental Monitoring and Assessment*, 174(1): 241-257.

Wang, J.P, Wang, X.J., and Zhang, J. (2013). Evaluating loss-on-ignition method for determinations of soil organic and inorganic carbon in arid soils of Northwestern China. *Pedosphere*, 23(5): 593-599.

Zárate, M.A., and Tripaldi, A. (2012). The aeolian system of central Argentina. *Aeolian Research*, 3(4): 401-417.

Zolitschka, B., Brauer, A., Negendank, J.F., Stockhausen, H., and Lang, A. (2000). Annually dated late Weichselian continental paleoclimate record from the Eifel, Germany. *Geology*, 28(9): 783-786.

Zougagh, M., Ríos, A., and Valcárcel, M. (2005). Direct determination of total carbonate salts in soil samples by continuous-flow piezoelectric detection. *Talanta*, 65(1): 29-35.